Since the energy contained within W_0 cannot exceed the total energy K_0, the upper bound of the average power in W_0 is K_0/D_0. Thus, the actual average power P_{W0} in W_0 of any signal $f \in \mathscr{C}$ can be written as

$$P_{W0} = (1{\cdot}25 + \zeta)P_{g0} \qquad |\zeta| \leq 0{\cdot}25 \quad (5)$$

Then P_{g0} is the guaranteed average power in W_0. It is worth noting that P_{W0} cannot exceed $1{\cdot}5P_{g0}$ and that the energy contained within W_0 is at least 2/3 of the total energy. From eqn. 5 a fair estimation of P_{W0} is derived as $\hat{P}_{W0} = 1{\cdot}20P_{g0}$, with a maximal error of 20% in the worst case. Note that with additional assumptions, the estimation can be refined further: for example, if the vertical line $t = t_0$ is an axis of symmetry of $f^2(t)$ and if $f^2(t)$ is a nonincreasing function for $t > t_0$, then $\tau_0 = t_0$ and a tighter estimation of P_{W0} can be derived as $\hat{\hat{P}}_{W_0} = 1{\cdot}38P_{g0}$ with a maximal error of 8% since, in this particular case, it can be shown that the energy contained in W_0 is at least 23/27 of the total energy.

In short, given an arbitrary signal $f \in \mathscr{C}$ with known energy K_0 and known moments K_1 and K_2, the segment of $f(t)$ which has the greater guaranteed average power is $f_{W0}(t)$. The length of this segment is a natural measure of the signal duration; thus we propose defining the effective duration of a signal $f \in \mathscr{C}$ by the length of its optimum window, i.e.

$$D_{eff} = 2\lambda_0 = 2\sqrt{(3)}\sigma \quad (6)$$

Now, defining the effective amplitude A_{eff} of $f \in \mathscr{C}$ as the height of a rectangular pulse of duration D_{eff} and energy K_0, we obtain

$$A_{eff} \triangleq [K_0/(2\lambda_0)]^{1/2} \quad (7)$$

Illustrative examples: Let $f(t)$ be a pulse of width T_0 shaped as a rectangle of height A. It is a simple matter to evaluate the three integrals K_i and then using eqns. 6 and 7 one obtains $D_{eff} = T_0$ and $A_{eff} = A$, which is a noteworthy property. A similar property holds in the discrete case; let $f(nT)$ be the sample values of a rectangular pulse defined by $f(nT) = A$ if $1 \leq n \leq N$; $f(nT) = 0$ otherwise. In this discrete case, the scalar products K_i are evaluated using definition eqn. 1*b*; eqns. 6 and 7 yield $D_{eff} = T\sqrt{(N^2 - 1)}$ and $A_{eff} = A[N/\sqrt{(N^2 - 1)}]^{1/2}$. Thus, provided the number of samples is not too small, $D_{eff} \simeq NT$ and $A_{eff} \simeq A$ as in the continuous case.

Let $f(t) = A \sin \pi t$ if $0 \leq t \leq T_0$; $f(t) = 0$ otherwise. Assuming for the sake of simplicity that T_0 is an integer, one obtains $D_{eff} = T_0/\eta^2$ and $A_{eff} = \eta[A/\sqrt{(2)}]$, with $\eta = [1 - 6/(\pi T_0)^2]^{-1/4}$; thus as T_0 increases, η comes very close to unity and another noticeable property is that the proposed effective amplitude A_{eff} gives for a time-limited sine wave a measure that is very close to the well known RMS value of an endless sine wave.

Consider now the one-sided exponential signal $f(t) = A\theta^{-t/\theta}$ defined over $[0, \infty[$. It is a simple matter to show that $D_{eff} = \theta\sqrt{(3)}$ and $A_{eff} = A[\sqrt{(3)/6}]^{1/2} \simeq 0{\cdot}537A$. An attractive feature of the new concept of effective amplitude lies in its ability to give an objective measure of transients. In problems dealing with least-squares approximation, we have found that the effective amplitude of the error is a meaningful and objective measure of goodness of fit.

It is felt that the optimal property derived in this letter could serve as a unifying basis for defining effective duration and effective amplitude, for both continuous and discrete signals.

L.C. CALVEZ
P. VILBE
J. C. BOULBRY

Laboratoire d'Electronique et Systèmes de Télécommunications (LEST)
URA CNRS n. 1329, Faculté des Sciences et Techniques
Université de Bretagne Occidentale (UBO)
6 avenue Le Gorgeu, 29287 Brest Cedex, France

19th July 1989

References

1 VILBE, P., and CALVEZ, L. C.: 'Constrained l_2 suboptimal model reduction', *Electron. Lett.*, 1987, **23**, pp. 1340–1342
2 ZAKIAN, V.: 'Relation between system parameters and response duration', *ibid.*, 1965, **1**, pp. 293–294
3 HELSTROM, C. W.: 'Statistical theory of signal detection' (Pergamon, 1968, 2nd edn.), p. 19
4 ROUBINE, E.: 'Introduction à la théorie de la communication, tome 1 (signaux non aléatoires)' (Masson, Paris, 1970)
5 PAPOULIS, A.: 'Signal analysis' (McGraw-Hill, NY, 1977)
6 ISHII, R., and FURUKAWA, K.: 'The uncertainty principle in discrete signals', *IEEE Trans.*, 1986, **CAS-33**, pp. 1032–1034

CHARACTERISTICS OF *p*-Ge/*N*-GaAs HETEROJUNCTIONS GROWN BY MOLECULAR BEAM EPITAXY

Indexing terms: Semiconductor devices and materials, Semiconductor junctions, Semiconductor growth, Epitaxy

We report the nearly ideal electrical characteristics of *p*-Ge/*N*-GaAs heterojunction diodes grown by molecular beam epitaxy. The temperature and device size dependencies of the current–voltage characteristics have been investigated. At room temperature, unity ideality factor has been demonstrated over almost six decades of current.

Germanium has a higher hole mobility and can be doped more heavily than any other device grade semiconductor. The nearly perfect lattice match to GaAs ($\approx 0{\cdot}1\%$) makes Ge an excellent candidate for optimising GaAs–AlGaAs devices by offering an additional degree of freedom in the design. The smaller bandgap of Ge suggests applications in hole-based modulation doped structures, GaAs–Ge quantum confinement structures, and phototransistors.[1] Further, heavily doped Ge could be used as a low bandgap, low resistance base for heterojunction bipolar transistors.[2,3] Defect-free Ge has recently been observed to grow epitaxially on GaAs(100),[4–7] but these reports did not emphasise the electrical properties of the Ge/GaAs heterojunction. In this letter we report the nearly ideal electrical characteristics of *p*-Ge/*N*-GaAs heterojunction diodes as a function of temperature. The influence of device size on the current–voltage characteristics was also investigated.

The GaAs growth was carried out in a Perkin Elmer 430 molecular beam epitaxy (MBE) system and Ge deposition took place in an adjacent chamber to minimise cross-contamination. Samples remained under vacuum during the several minutes of growth interruption required to transfer samples between chambers. All sources were solid-source effusion cells. An initial buffer layer of 1 μm Si-doped GaAs was grown with a carrier concentration of $N = 4 \times 10^{18}\,cm^{-3}$ on a semi-insulating GaAs(100) substrate. Next, 0·4 μm of GaAs was deposited with a lighter Si doping of $N = 7 \times 10^{16}\,cm^{-3}$. Finally, 500 Å of Ge was grown, the growth being interrupted three times for Ga delta doping to a hole concentration of $p \approx 1 \times 10^{19}\,cm^{-3}$.

After growth, diodes with various mesa sizes were fabricated by standard photolithographic and wet etching techniques. The *n*-type contacts were formed by evaporating AuGe/Ni/Au on n^+-GaAs and alloying at 450°C. Chemical palladium plating was employed for the *p*-type contact on Ge. Both *n* and *p*-type contacts were verified to be ohmic with corresponding contact resistances of $1{\cdot}6 \times 10^{-6}$ and $7{\cdot}5 \times 10^{-6}\,\Omega\,cm^2$, respectively.

Fig. 1 shows a typical room-temperature current–voltage (I/V) characteristics of a *p*-Ge/*N*-GaAs heterojunction diode. As can be seen, the diode exhibits a sharp turn-on at about 0·4 V and low reverse bias leakage with a breakdown at ≈ 8 V.

Shown in Fig. 2 are I/V characteristics at various temperatures. We observe a shift to higher voltages at given current levels as temperature decreases. This is an expected consequence of higher turn-on voltage at lower temperatures. However, general characteristics of the I/V curves do not change with the temperature. All exhibit a constant slope (constant ideality factor) in the low-current regime. At higher current levels, the curves eventually saturate due to the series resistance associated with the metal contacts.

For a quantitative comparison of the current mechanisms, Table 1 lists the ideality factors n and corresponding logarithmic slope constants ($\alpha = q/nkT$) as measured at various temperatures. At room temperature, the ideality factor is 1·02, and as can be seen from Fig. 2, the minimum ideality factor region extends over almost 5 decades of current density. Even larger current ranges (six decades) of minimum ideality factor was demonstrated for smaller size diodes. The nearly ideal I/V characteristics suggest that the current is due purely to diffusion, and there exists a very marginal loss through space charge recombination. Surface recombination is further studied through I/V characterisation of different size diodes. Over two orders of magnitude of device area range, I/V characteristics were very similar with ideality factors from 1·00 to 1·15.

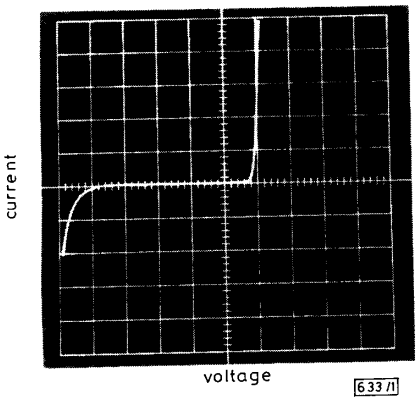

Fig. 1 *Typical room-temperature current/voltage characteristics of p-Ge/N-GaAs heterojunction*
Forward bias: 0·5 V/div, 0·5 mA/div.
Reverse bias: 2 V/div, 2 mA/div

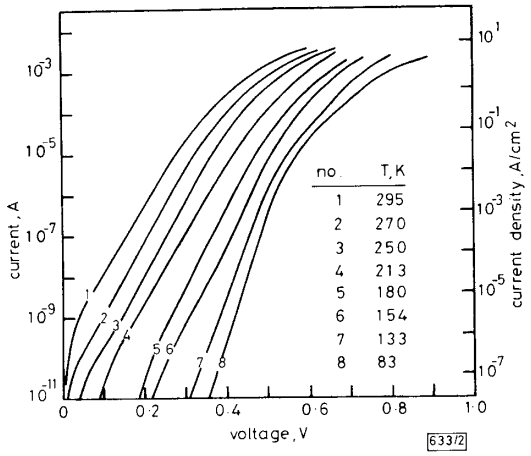

Fig. 2 *Temperature dependence of I/V characteristics of p-Ge/N-GaAs diodes*

Table 1 shows that the ideality factor slowly increases with decreasing temperatures. This increase is very uniform and does not exhibit sharp changes. The highest ideality factor 1·94 is obtained at 83 K. Since the ideality factor stays below 2 for all temperatures and the I/V characteristics do not exhibit significant changes with the temperature, we believe that the main transport is by diffusion, even at low temperatures. The increase in the ideality factor with decreasing temperature is attributed to the effect of the potential spike resulting from conduction band discontinuity at the abrupt GaAs/Ge interface and recombination current component. As the temperature decreases, tunnelling and recombination components become more significant compared to decreasing diffusion current resulting in higher ideality factors.

In conclusion, we have studied the I/V characteristics of the p-Ge/N-GaAs diode. Nearly ideal behaviour suggests an almost unhindered injection of electrons from N-GaAs to p-Ge; the hole transport from p-Ge to N-GaAs can be neglected due to a relatively large valence band discontinuity. The p-Ge/N-GaAs system is very promising and can successfully be incorporated in high-performance heterojunction bipolar transistors.

Table 1

T	n	α
K		
295	1·02	38·4
270	1·04	41·2
250	1·11	41·6
213	1·36	40·0
180	1·44	44·6
154	1·54	48·8
113	1·61	54·1
83	1·94	72·0

This research is supported by the Air Force Office of Scientific Research (grant AFOSR-89-0239) and by the SDIO IST Office through ONR (grant N00014-86-K-0513). One of us (SS) wishes to acknowledge the support of an NSF graduate fellowship.

M. S. ÜNLÜ
S. STRITE
T. WON
K. ADOMI
J. CHEN
S. NOOR MOHAMMAD
D. BISWAS
H. MORKOÇ

Material Science Laboratory and Coordinated Science Laboratory
University of Illinois at Urbana-Champaign
1101 W. Springfield Avenue, Urbana, IL 61801, USA

3rd August 1989

References

1 CHAND, N., KLEM, J., and MORKOÇ, H.: 'Pnp GaAs/Ge/Ge phototransistor grown by molecular beam epitaxy: Implications for bipolar and hot electron transistors', *Appl. Phys. Lett.*, 1986, **48**, pp. 484–486
2 JADUS, D. K., and FEUCHT, D. L.: 'The realization of a GaAs–Ge wide band gap emitter transistor', *IEEE Trans. Electron Dev.*, 1969, **ED-16**, pp. 102–107
3 KIMURA, T., KAWANAKA, M., and SONE, J.: 'MBE-grown Ge/GaAs heterojunction bipolar transistors operated at 300 K and 77 K with current gain of 45'. Paper IIA-8, 47th Device Research Conference, 19th–21st June 1989, Cambridge, MA, IEEE
4 BAUER, R. S., and MIKKELSON, J. C.: 'Surface processes controlling MBE heterojunction formation: GaAs(100)/Ge interfaces', *J. Vac. Sci. Technol.*, 1982, **21**, pp. 491–496
5 CHANG, C.-A.: 'Interface morphology of epitaxial growth of Ge on GaAs and GaAs on Ge by molecular beam epitaxy', *J. Appl. Phys.*, 1982, **53**, pp. 1253–1255
6 NEAVE, J. H., LARSEN, P. K., JOYCE, B. A., GOWERS, J. P., and VAN DER VEEN, J. F.: 'Some observations on Ge : GaAs(001) and GaAs : Ge(001) interfaces and films', *J. Vac. Sci. Technol.*, 1983, **B1**, pp. 668–674
7 STRITE, S., BISWAS, D., KUMAR, N. S., FRADKIN, M., and MORKOÇ, H.: 'Antiphase domain free growth of GaAs on Ge in GaAs/Ge/GaAs heterostructures', submitted to *Appl. Phys. Lett.*

WAVELENGTH CONVERSION FOR FM LIGHT USING LIGHT INJECTION INDUCED FREQUENCY SHIFT IN DFB-LD

Indexing terms: Optics, Optical communications, Convertors, Optical filters

A novel wavelength conversion is described. Wavelength conversion of frequency-modulated (FM) light is achieved by combining the lasing frequency shift induced by external light in a DFB-LD and the FM–IM conversion function of a Mach–Zehnder optical filter. In the experiment, 1534 nm FM light is converted to 1550 nm light.

Introduction: Wavelength convertors are desirable for future lightwave systems, since they can enable us to construct flex-